

Magnetized accretion disks around Kerr black holes with scalar hair - I. Constant angular momentum

Sergio Gimeno-Soler,¹ José A. Font,^{1,2} Carlos Herdeiro,³ and Eugen Radu³

¹*Departamento de Astronomía y Astrofísica, Universitat de València,
Dr. Moliner 50, 46100, Burjassot (València), Spain*

²*Observatori Astronòmic, Universitat de València,
C/ Catedrático José Beltrán 2, 46980, Paterna (València), Spain*

³*Departamento de Física da Universidade de Aveiro and CIDMA, Campus de Santiago, 3810-183 Aveiro, Portugal*

(Dated: June 25, 2018)

We present a method to build magnetized constant angular momentum disks around Kerr black holes with scalar hair (KBHsSH).

PACS numbers: 95.30.Sf, 04.70.Bw, 04.40.Nr, 04.25.dg

I. INTRODUCTION

II. FRAMEWORK

We use the stationary and axisymmetric metric ansatz provided by[1]

$$ds^2 = e^{2F_1} \left(\frac{dr^2}{N} + r^2 d\theta^2 \right) + e^{2F_2} r^2 \sin^2 \theta (d\phi - W dt)^2 - e^{2F_0} N dt^2, \quad (1)$$

with $N = 1 - r_H/r$, where r_H is the radius of the event horizon of the BH and W, F_1, F_2, F_0 are functions of r and θ .

This metric is a solution to the Einstein-Klein-Gordon field equations $R_{ab} - \frac{1}{2}Rg_{ab} = 8\pi G(T_{SF})_{ab}$ with

$$(T_{SF})_{ab} = \partial_a \Psi^* \partial_b \Psi + \partial_b \Psi^* \partial_a \Psi - g_{ab} \left(\frac{1}{2} g^{cd} (\partial_c \Psi^* \partial_d \Psi + \partial_d \Psi^* \partial_c \Psi) + \mu^2 \Psi^* \Psi \right), \quad (2)$$

where Ψ is a complex Klein-Gordon field such as $\Psi = \phi(r, \theta) e^{im\phi - wt}$ where w is the scalar field frequency and m is the azimuthal harmonic index. Details about the obtention of the solution and the behaviour of the metric functions W, F_i are presented in [2].

A. Distribution of angular momentum and equations of motion

We introduce the specific angular momentum l and the angular velocity Ω employing the standard definitions,

$$l = -\frac{u_\phi}{u_t}, \quad \Omega = \frac{u^\phi}{u^t}, \quad (3)$$

where u^μ is the fluid four-velocity. The relationship between l and Ω is given by the equations

$$l = -\frac{\Omega g_{\phi\phi} + g_{t\phi}}{\Omega g_{t\phi} + g_{tt}}, \quad \Omega = -\frac{l g_{tt} + g_{t\phi}}{l g_{t\phi} + g_{\phi\phi}}, \quad (4)$$

where we are assuming circular motion, i.e. the four-velocity can be written as

$$u^\mu = (u^t, 0, 0, u^\phi). \quad (5)$$

We consider a constant angular momentum distribution $l(r, \theta) = \text{cte.}$. The specific value of the angular momentum is computed as the minimum of the following equation

$$l_b^\pm(r, \theta) = \frac{g_{t\phi} \pm \left(\sqrt{g_{t\phi}^2 - g_{tt}g_{\phi\phi}} \right) \sqrt{1 + g_{tt}}}{-g_{tt}} \quad (6)$$

where the plus sign is for prograde orbits and the minus is for retrograde orbits. This expression is given by [3] for Kerr BHs, but it is valid for any stationary, axisymmetric spacetimes. For prograde motion, the function has a minimum outside the event horizon. The location of said minimum corresponds with the marginally bound orbit r_{mb} , and the angular momentum corresponds to the keplerian angular momentum l_{mb} at that point. We show the proof of this statement at appendix B. This choice of angular momentum distribution is motivated by its simplicity (for a first study of thick tori around KBHsSH) and for allowing the presence of a cusp (to allow matter accretion onto the black hole) and a centre.

B. Magnetized disks

We use the procedure described by [4], where we write the equations of ideal general relativistic MHD as the following conservation laws, $\nabla_\mu T^{\mu\nu} = 0$, $\nabla_\mu {}^*F^{\mu\nu} = 0$, and $\nabla_\mu (\rho u^\mu) = 0$, where ∇_μ is the covariant derivative and

$$T^{\mu\nu} = (\rho h + b^2) u^\mu u^\nu + \left(p + \frac{1}{2} b^2 \right) g^{\mu\nu} - b^\mu b^\nu, \quad (7)$$

is the energy-momentum tensor of a magnetised perfect fluid, h , ρ p being the fluid specific enthalpy, density and fluid pressure, respectively. Moreover, ${}^*F^{\mu\nu} = b^\mu u^\nu - b^\nu u^\mu$ is the (dual of the) Faraday tensor relative

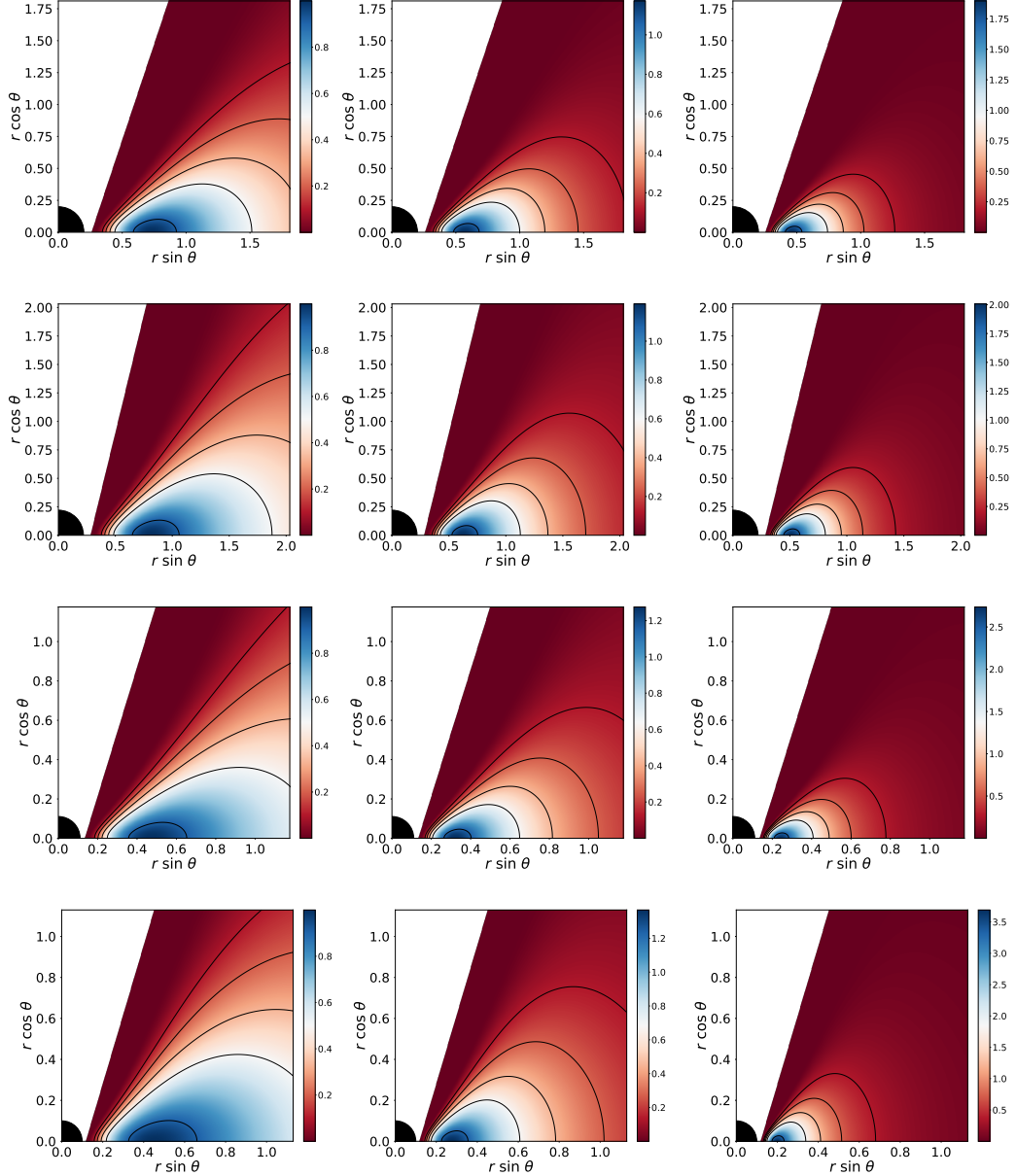


FIG. 1. Rest-mass density distribution. From top to bottom the rows correspond to the different models for the KBHsSH (I, II, III and IV). From left to right the columns correspond to different values of the magnetization parameter, namely non-magnetized ($\beta_{mc} = 10^{10}$), mildly magnetized ($\beta_{mc} = 1$) and strongly magnetized ($\beta_{mc} = 10^{-10}$)

to an observer with four-velocity u^μ , and b^μ is the magnetic field in that frame, with $b^2 = b^\mu b_\mu$. Assuming the magnetic field is purely azimuthal, i.e. $b^r = b^\theta = 0$, and taking into account that the flow is stationary and axisymmetric, the conservation of the current density and of the Faraday tensor follow. Contracting the divergence of Eq. (7) with the projection tensor $h^\alpha_\beta = \delta^\alpha_\beta + u^\alpha u_\beta$, we arrive at

$$(\rho h + b^2)u_\nu \partial_i u^\nu + \partial_i \left(p + \frac{b^2}{2} \right) - b_\nu \partial_i b^\nu = 0, \quad (8)$$

where $i = r, \theta$. Then, we rewrite this equation in terms of the specific angular momentum l and of the angular velocity Ω , to obtain

$$\partial_i (\ln u_t) - \frac{\Omega \partial_i l}{1 - l\Omega} + \frac{\partial_i p}{w} + \frac{\partial_i (\mathcal{L}b^2)}{2\mathcal{L}w} = 0, \quad (9)$$

where $\mathcal{L} = g_{t\phi}^2 - g_{tt}g_{\phi\phi}$.

To integrate Eq. (9) we first assume a polytropic equation of state of the form

$$p = K\rho^\Gamma, \quad (10)$$

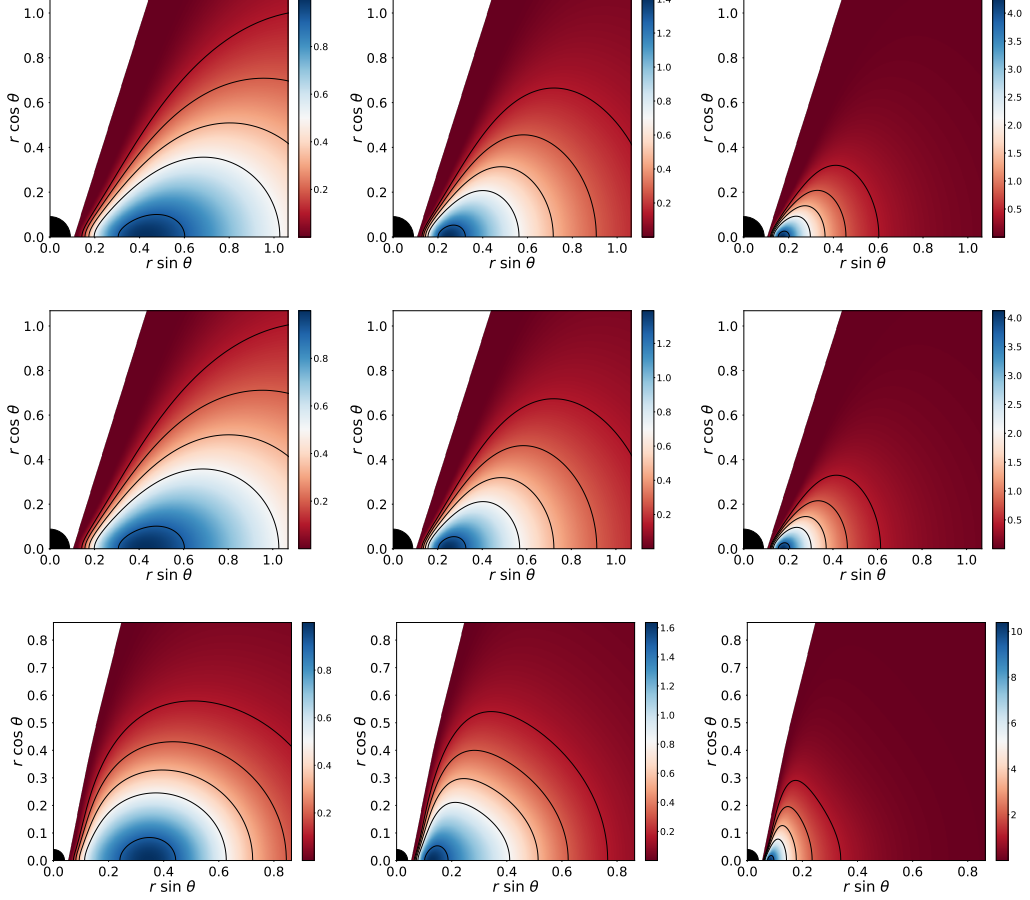


FIG. 2. Rest-mass density distribution. From top to bottom the rows correspond to the different models for the KBHsSH (V, VI and VII). From left to right the columns correspond to different values of the magnetization parameter, namely non-magnetized ($\beta_{mc} = 10^{10}$), mildly magnetized ($\beta_{mc} = 1$) and strongly magnetized ($\beta_{mc} = 10^{-10}$)

with K and Γ constants. Then, we define the magnetic pressure as $p_m = b^2/2$, the magnetization parameter $\beta_m = p/p_m$, and introduce the definitions $\tilde{p}_m = \mathcal{L}p_m$ and $\tilde{w} = \mathcal{L}w$, in order to write an analogous equation to Eq. (10) for \tilde{p}_m

$$\tilde{p}_m = M\tilde{w}^q, \quad (11)$$

or, in terms of the magnetic pressure p_m

$$p_m = M\mathcal{L}^{q-1}w^q, \quad (12)$$

where $w = \rho h$ is the fluid enthalpy density, and M and q are constants. If we define the potential as $W \equiv \ln|u_t|$, then we can integrate the equation (9) as

$$W - W_{in} + \ln \left(1 + \frac{\Gamma K}{\Gamma + 1} \rho^{\Gamma - 1} \right) + \frac{q}{q - 1} M(\mathcal{L}w)^{q-1} = 0, \quad (13)$$

where W_{in} is the potential at the inner edge of the disk.

We also write the expressions of the total energy density for the torus ρ_T :

$$\rho_T = -T_t^t + T_i^i = \frac{\rho h(g_{\phi\phi} - g_{tt}l^2)}{g_{\phi\phi} + 2g_{t\phi}l + g_{tt}l^2} + 2(p + p_m), \quad (14)$$

and the total energy density for the scalar field ρ_{SF} :

$$\rho_{SF} = -(T_{SF})_t^t + (T_{SF})_i^i = 2 \left(\frac{2e^{2F_0}w(w - mW)}{N} - \mu^2 \right) \phi^2. \quad (15)$$

In this work, we set the mass of the scalar field $\mu = 1$, the angular momentum to $l = l_{mb}$, the inner radius of the disk to $r_{in} = r_{mb}$, the exponents of the polytropic EoS to $q = \Gamma = 4/3$, and the density at the disk centre $\rho_c = 1$. Then, we leave the magnetization at the center β_{mc} as a parameter (for each model of KBHSH). With this information we can compute all the relevant physical quantities.

III. METHOD

A. Building the disk

To construct our models we take the following steps: First, we find the angular momentum l and the radius of the cusp r_{cusp} as the value at the minimum and the

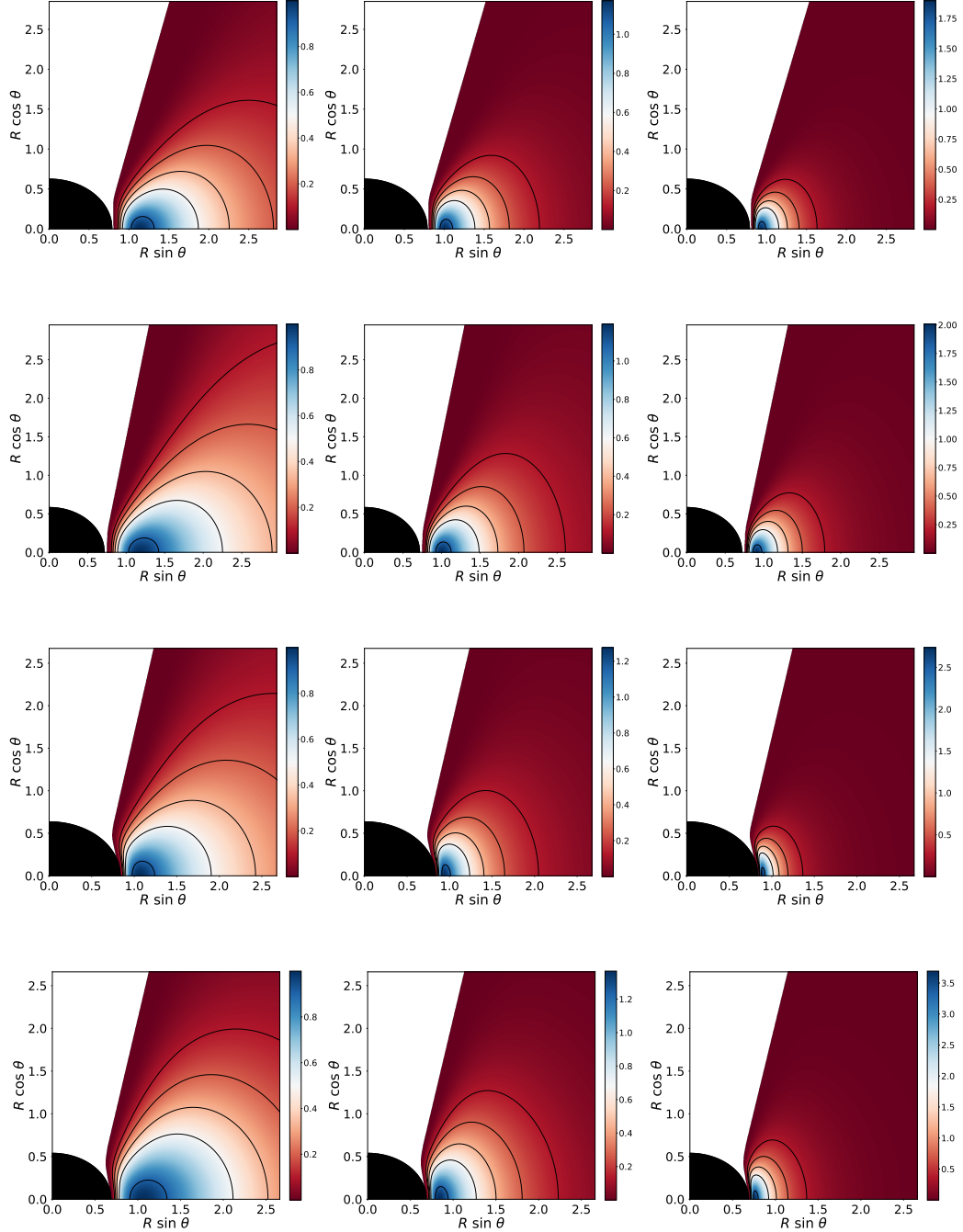


FIG. 3. Rest-mass density distribution using perimeteral coordinates. From top to bottom the rows correspond to the different models for the KBHsSH (I, II, III and IV). From left to right the columns correspond to different values of the magnetization parameter, namely non-magnetized ($\beta_{m_c} = 10^{10}$), mildly magnetized ($\beta_{m_c} = 1$) and strongly magnetized ($\beta_{m_c} = 10^{-10}$)

location of said minimum outside the event horizon of equation (6). This choice of angular momentum implies $r_{\text{cusp}} = r_{\text{mb}}$, $l = l_K(r_{\text{mb}})$ and $W_{\text{in}} = 0$ and then, we can compute the potential distribution as $W(r, \theta) \equiv \ln |u_t|$. Considering this, and that we can write the magnetic

pressure at the center as

$$p_{m_c} = M \mathcal{L}^{q-1} \left(1 + \frac{\Gamma K}{\Gamma + 1} \right)^q = K / \beta_{m_c}, \quad (16)$$

where we have taken into account that $\rho_c = 1$, that the pressure at the center is $p_c = K$ and the specific enthalpy

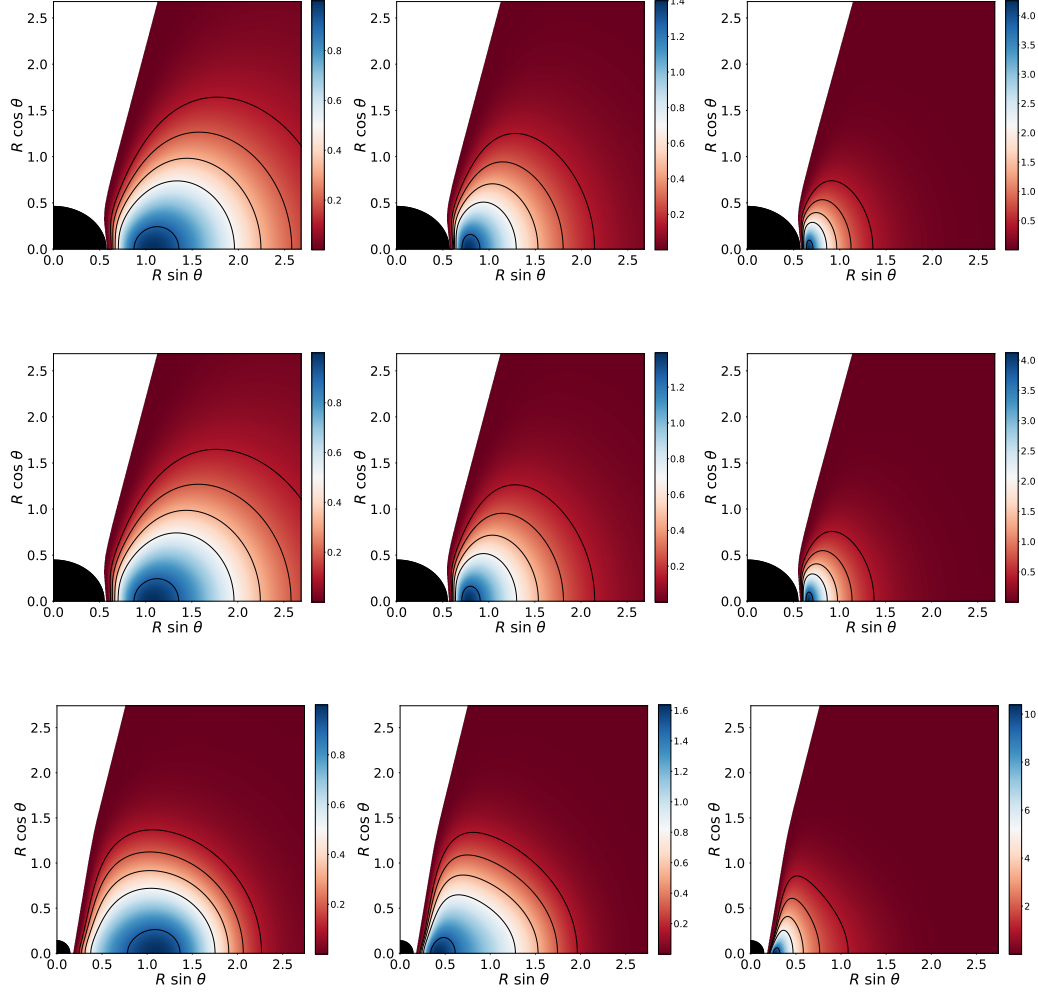


FIG. 4. Rest-mass density distribution using perimetal coordinates. From top to bottom the rows correspond to the different models for the KBHsSH (V, VI, VII). From left to right the columns correspond to different values of the magnetization parameter, namely non-magnetized ($\beta_{mc} = 10^{10}$), mildly magnetized ($\beta_{mc} = 1$) and strongly magnetized ($\beta_{mc} = 10^{-10}$)

can be written as $h = 1 + \frac{\Gamma K}{\Gamma+1} \rho^{\Gamma-1}$. Replacing this into the equation (13) we arrive at an equation for the polytropic constant K

$$W_c + \ln \left(1 + \frac{\Gamma K}{\Gamma+1} \right) + \frac{q}{q-1} \frac{K/\beta_{mc}}{1 + \frac{\Gamma K}{\Gamma+1}} = 0. \quad (17)$$

Once we have K , it is easy to find p_m , M and h_c with the definition of the magnetization parameter at the center β_{mc} , the equation (12) and $h = 1 + \frac{\Gamma K}{\Gamma+1} \rho^{\Gamma-1}$. With this, we already have all we need in order to compute all the relevant physical quantities inside the disk.

B. Numerical method

We start from a uniform numerical grid (X, θ) (with x being a compactified radial coordinate such as $X =$

$x/(1+x)$ and $x = \sqrt{r^2 - r_H^2}$) with a domain $[0, 1] \times [0, \pi/2]$ and a number of points of $N_X \times N_\theta = 251 \times 30$. Then, we transform and interpolate the grid to end with a non-uniform grid (r, θ) with a domain $[r_H, 199.2] \times [0, \pi/2]$ and a number of points $N_r \times N_\theta = 2500 \times 300$, this is the grid we use for our computations.

IV. RESULTS

In table I we show the different KBHsSH models we will use. As it can be seen, the models go from a Kerr-like model (almost all the mass and angular momentum are stored in BH) to a KBHSH with almost all the mass and angular momentum stored in the scalar field. It is also worth mentioning that, as shown in table II some of the models violate the Kerr bound (in terms of ADM or horizon quantities). This is not worrying because, as

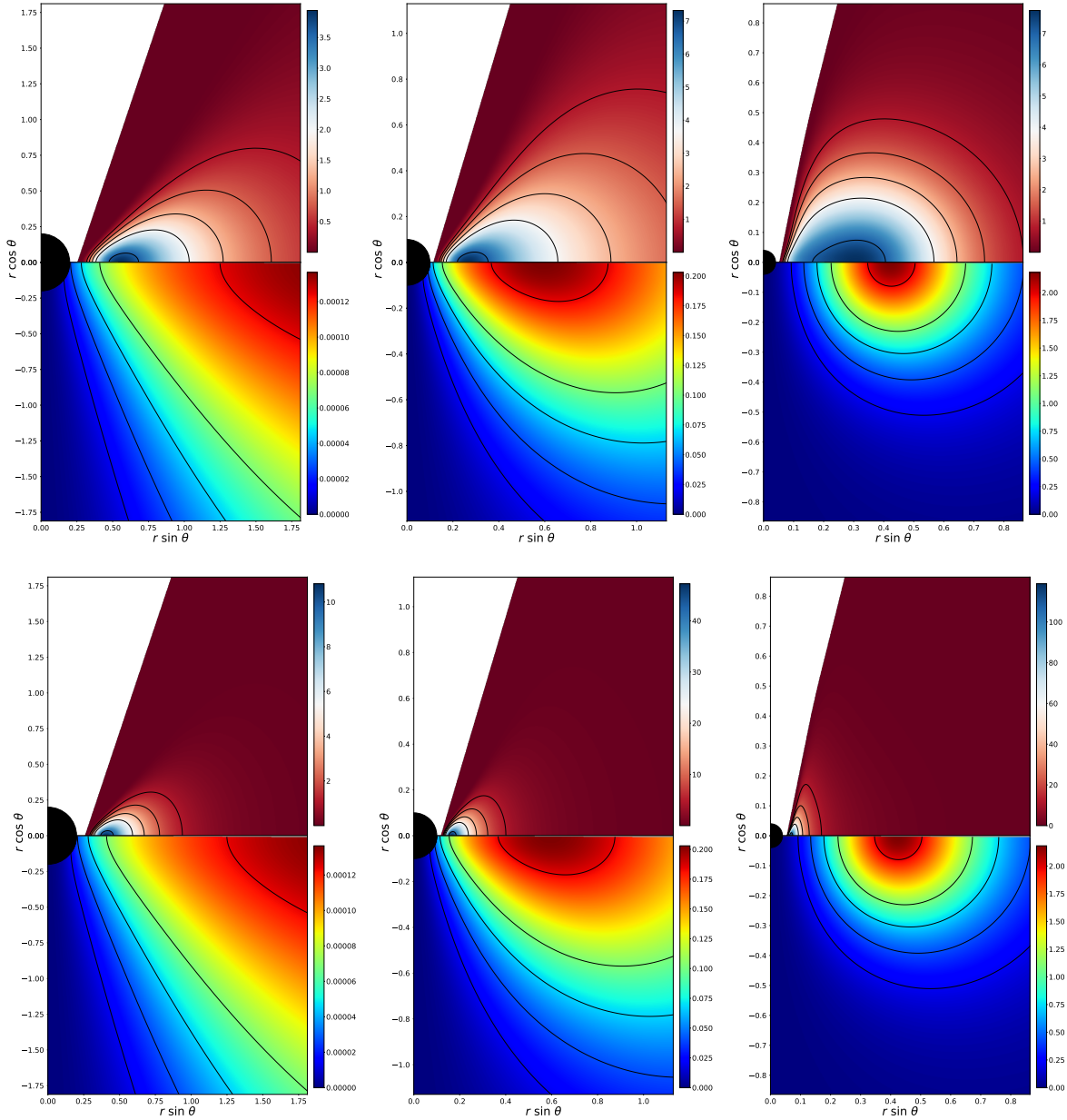


FIG. 5. Gravitational mass density distribution for the torus ρ_T (up) and the scalar field ρ_{SF} (down). From left to right the columns correspond to different models (I, IV and VII). From top to bottom, the rows correspond to different values of the magnetization parameter, namely non-magnetized ($\beta_{m_c} = 10^{10}$) and strongly magnetized ($\beta_{m_c} = 10^{-10}$)

shown in [5] the horizon linear velocity v_H never exceed 1. For comparison, we also show the spin parameter $a_{H_{eq}}$ corresponding to a Kerr BH with horizon linear velocity v_H .

In figures 1 and 2 we show the rest-mass density distribution for all our KBHsSH models with 3 different values of the magnetization parameter at the center β_{m_c} , namely 10^{10} , 1 and 10^{-10} . In figures 3 and 4 we show the same models, but using a perimetral radial coordinate such as $R = e^{F_2}r$. Also, in figures 9 and 10 we show different KBH models with the same mass $M_{BH} = 1$

and different values for the spin parameter(0, 0.5, 0.9, 0.9999). Tables III and IV show the relevant physical quantities for both KBHsSH and the same KBH cases we presented in the figures. First of all, it is worth to mention that KBHsSH can violate the Kerr bound for the potential $\Delta W \equiv W_{in} - W_c$. As shown in [6], constant angular momentum disks exhibit a maximum for $|\Delta W|$ when the spin parameter a approaches 1. This value is $\Delta W_{max} = -\frac{1}{2} \ln 3 \simeq -0.549$. The models V, VI and VII violate that bound. This is related, as we will see, with the maximum value of the specific enthalpy, pressure and

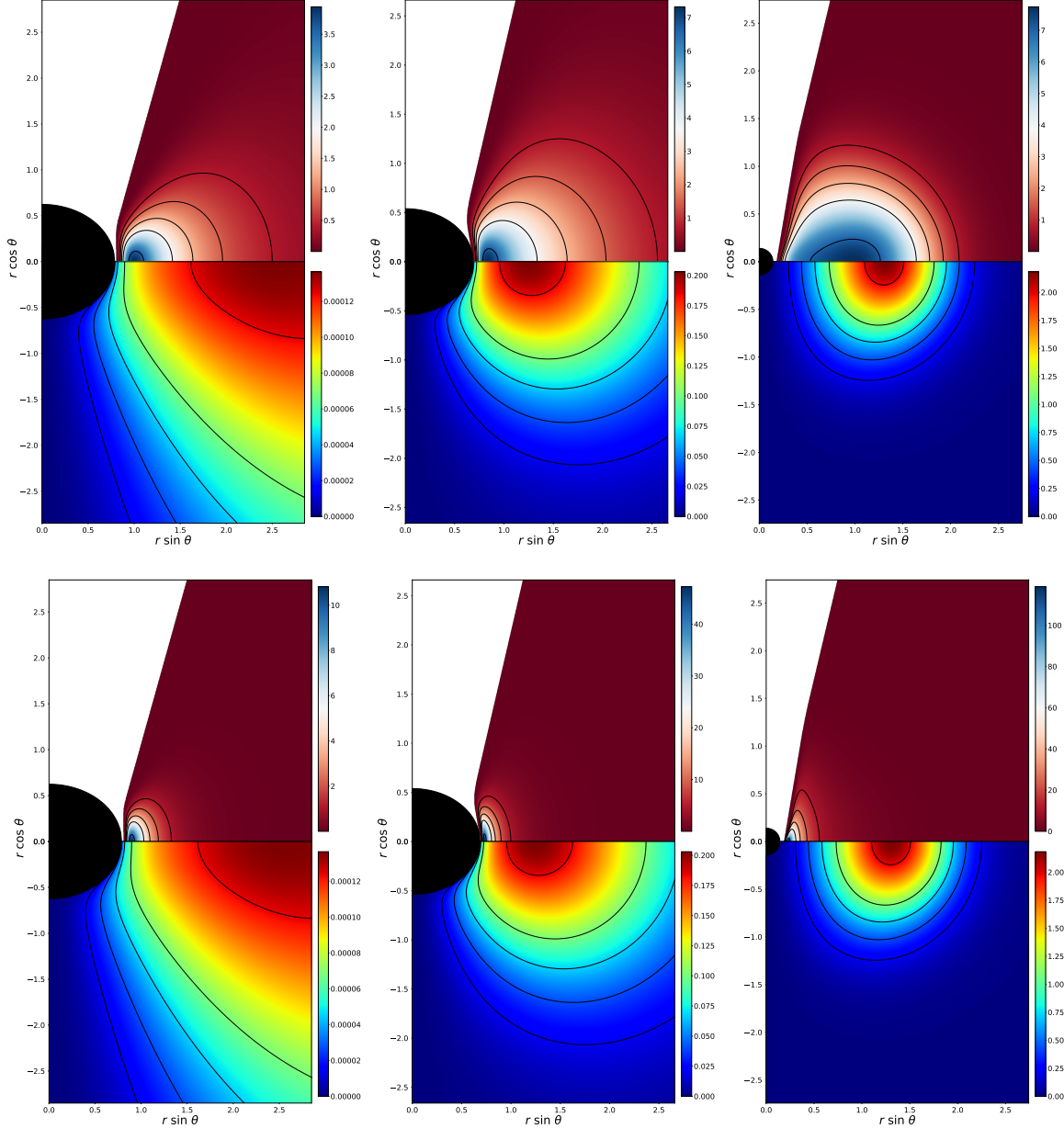


FIG. 6. Gravitational mass density distribution for the torus ρ_T (up) and the scalar field ρ_{SF} (down) using perimetral coordinates. From left to right the columns correspond to different models (I, IV and VII). From top to bottom, the rows correspond to different values of the magnetization parameter, namely non-magnetized ($\beta_{mc} = 10^{10}$) and strongly magnetized ($\beta_{mc} = 10^{-10}$)

magnetic pressure.

In figure 5 we show the total energy density of the torus ρ_T (superior half) and the total energy density of the scalar field ρ_{SF} for 3 of the models (I, IV and VII) and 2 values of the magnetization parameter at the center (10^{10} and 10^{-10}). In figure 6, we show the same, but using the perimetral coordinate we defined earlier. The plots show that the maximum of the total energy density of the disk ρ_t is closer to the maximum of the total energy density of the scalar field ρ_{SF} for increasing hair.

The behaviour of the maximum specific enthalpy h_{\max} and the maximum rest-mass density ρ_{\max} is shown in figures 7 for the models (I-VII) and for a sequence of increasing spin parameter KBHs, here we can see that, for both cases, an increase in $|\Delta W|$ implies higher values for h_{\max} (low magnetization) and also higher values for ρ_{\max} (high magnetization). However, there are differences between the two cases. For the enthalpy, the values of h_{\max} reached for the KBHsSH are much higher than those of the KBH case. This fact tells us that,

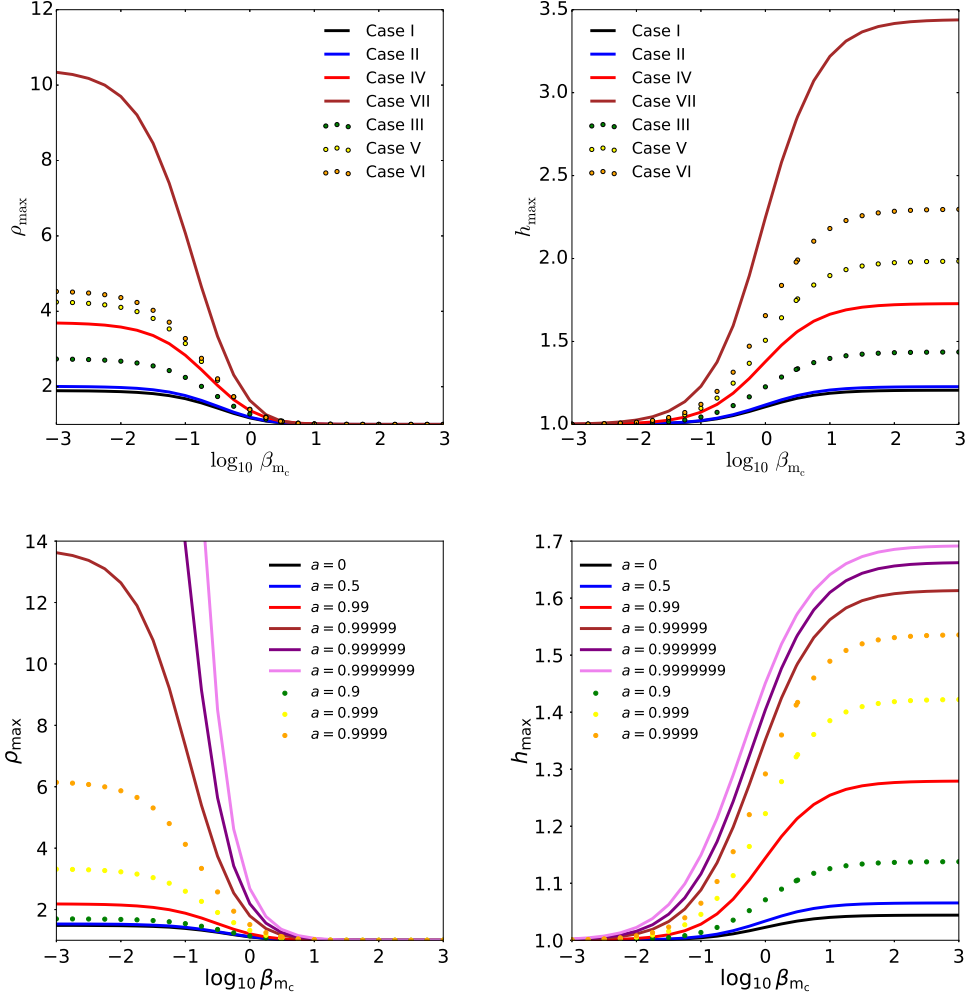


FIG. 7. Effects of the magnetization on the values for the maximum density (left) and enthalpy (right) of the disc. In the first row, we show this for all of our KBHsSH models. In the second row, we show this for a sequence of KBHs with increasing spin parameter.

while the $w = \rho h \simeq \rho$ approximation (see [7] and [8]) is valid for magnetized flows ($\beta_{m_c} \sim 1$) for reasonable values of the spin parameter ($a \sim 0.99$ or lower), that is not the case for KBHsSH. Also, for the rest-mass density we have a different behaviour: ρ_{\max} for KBHsSH reach values only attainable by high spin parameter KBHs (between $a = 0.9$ and $a = 0.99999$ for the seven models we present here).

Figure 8 shows the variation of the quotient of the perimetal radius of the magnetic pressure maximum by the perimetal radius of the disk center $R_{m,\max}/R_c$ with the decimal logarithm of the magnetization parameter at the disk center $\log_{10} \beta_{m_c}$ for the same KBHsSH and KBH cases as in figure 7. The inset shows a region around $\beta_{m_c} = 3$ and $R_{m,\max}/R_c = 1$, this is because for disks with $h = 1$, $R_{m,\max} = R_c$ if $\beta_{m_c} = 1/\Gamma - 1$. As we can easily see, this condition is also fulfilled for the Kerr case, even $h \neq 1$ (with a slight deviation for very high

spin parameter cases), but not quite for the KBHsSH cases.

SG: Include discussion about radial profiles.

As shown in [9] some SG: (compute which ones are embeddable and which are not) of our models are in the region of the domain of existence where the event horizon is not embeddable in \mathbb{E}^3 then, the shaded regions depicting the horizon that we show at several of the figures are not faithful representations of the horizon geometry. Nevertheless, we show them for the sake of clarity. Also, this led us to asking ourselves if this could also happen for the shape of the accretion tori and therefore, we should be conservative when extracting information about the morphology of the disks from 2-dimensional plots. This idea is discussed in appendix A.

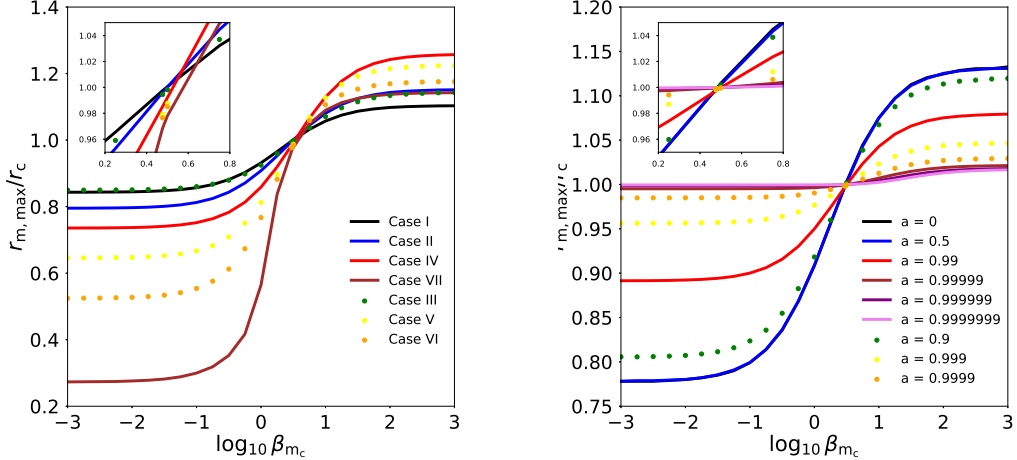


FIG. 8. Effects of the magnetization on the (perimeteral) location of the magnetic pressure maximum (divided by the the perimeteral radius of the centre) $(R_{\text{mag},\max}/R_c)$. Left panel: KBHsSH models. Right panel: A sequence of KBHs with increasing spin parameter.

TABLE I. List of models of KBHsSH.

Model	M_{ADM}	J_{ADM}	M_H	J_H	M_{SF}	J_{SF}	r_H
I	0.415	0.172	0.393	0.15	0.022	0.022	0.2
II	0.630	0.403	0.340	0.121	0.063	0.282	0.221
III	0.797	0.573	0.365	0.172	0.573	0.432	0.111
IV	0.933	0.739	0.234	0.114	0.699	0.625	0.1
V	0.940	0.757	0.159	0.076	0.757	0.781	0.091
VI	0.959	0.795	0.087	0.034	0.872	0.781	0.088
VII	0.975	0.85	0.018	0.002	0.957	0.848	0.04

TABLE II. Values of the normalized spin parameter for the ADM quantities (a_{ADM}), for the BH horizon quantities (a_H), the horizon linear velocity (v_H) and the spin parameter corresponding to a KBH with a linear velocity equal to v_H , ($a_{H_{\text{eq}}}$).

Model	a_{ADM}	a_H	v_H	$a_{H_{\text{eq}}}$
I	0.9987	0.9712	0.7685	0.9663
II	1.014	0.3760	0.6802	0.9301
III	0.9032	1.295	0.7524	0.9608
IV	0.8489	2.082	0.5635	0.8554
V	0.8560	3.017	0.4438	0.7415
VI	0.9477	3.947	0.2988	0.5487
VII	0.8941	6.173	0.09732	0.1928

V. CONCLUSIONS

Future work: Non-constant angular momentum case, Proca hair, shadows of the system HBH+disk.

ACKNOWLEDGMENTS

-
- [1] C. A. R. Herdeiro and E. Radu, Physical Review Letters **112**, 221101 (2014), arXiv:1403.2757 [gr-qc].
[2] C. Herdeiro and E. Radu, Classical and Quantum Gravity **32**, 144001 (2015), arXiv:1501.04319 [gr-qc].
[3] F. Daigne and J. A. Font, MNRAS **349**, 841 (2004), astro-ph/0311618.
[4] P. J. Montero, O. Zanotti, J. A. Font, and L. Rezzolla, MNRAS **378**, 1101 (2007), astro-ph/0702485.
[5] C. A. R. Herdeiro and E. Radu, International Journal of Modern Physics D **24**, 1544022 (2015), arXiv:1505.04189 [gr-qc].

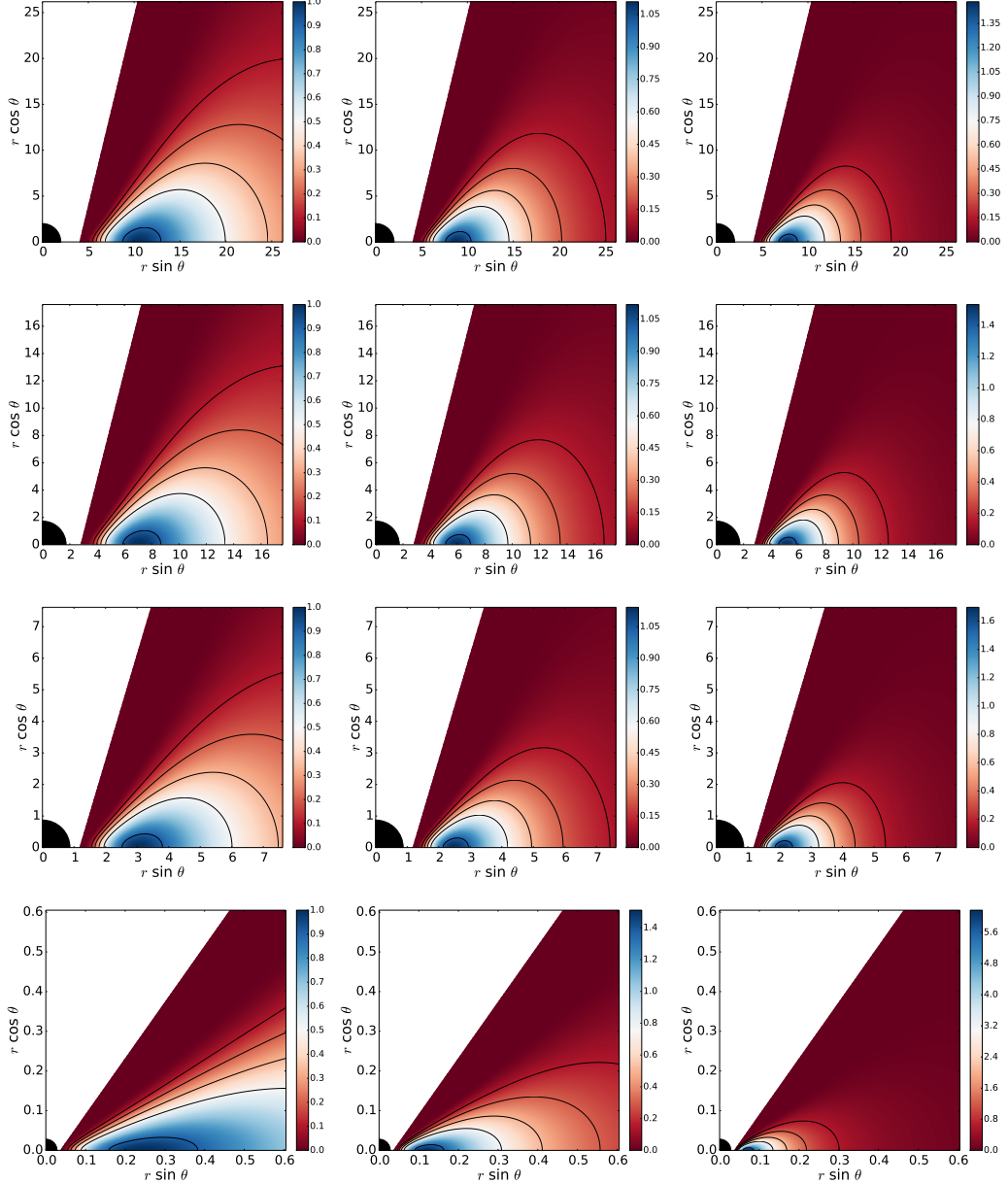


FIG. 9. Rest-mass density distribution. From top to bottom the rows correspond to a sequence of KBHs with increasing spin parameter a (0, 0.5, 0.9 and 0.9999). From left to right the columns correspond to different values of the magnetization parameter, namely non-magnetized ($\beta_{mc} = 10^{10}$), mildly magnetized ($\beta_{mc} = 1$) and strongly magnetized ($\beta_{mc} = 10^{-10}$)

- [6] M. Abramowicz, M. Jaroszynski, and M. Sikora, *A&A* **63**, 221 (1978).
- [7] S. S. Komissarov, *MNRAS* **368**, 993 (2006), astro-ph/0601678.
- [8] S. Gimeno-Soler and J. A. Font, *Astron. Astrophys.* **607**, A68 (2017), arXiv:1707.03867 [gr-qc].
- [9] J. F. M. Delgado, C. A. R. Herdeiro, and E. Radu, ArXiv e-prints (2018), arXiv:1804.04910.

Appendix A: Embedding of the accretion torus in \mathbb{E}^3

Following the same reasoning as in [9], we write the 2-metric for the surface of a torus as

$$d\sigma^2 = \frac{e^{2F_1}}{N} dr^2 + e^{2F_1} r^2 d\theta^2 + e^{2F_2} r^2 \sin^2 \theta d\phi^2, \quad (\text{A1})$$

and the condition $r = r(\theta)$ for the surface of the torus. The location of the surface of the torus $r(\theta)$ can be obtained integrating $r' = \frac{dr}{d\theta} = -\frac{\partial_\theta W}{\partial_r W}$ (equation (24) of [8]).

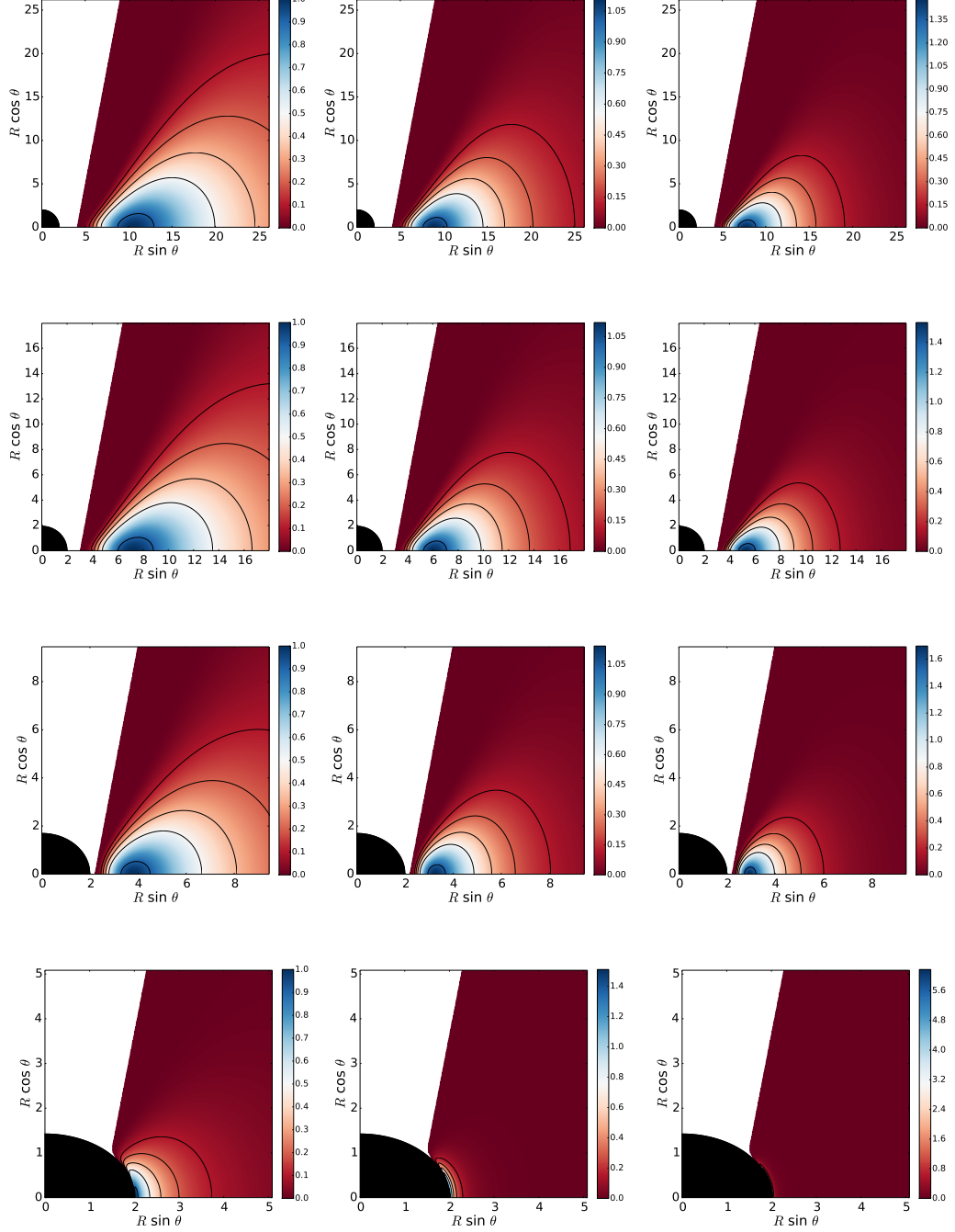


FIG. 10. Rest-mass density distribution using perimetric coordinates. From top to bottom the rows correspond to a sequence of KBHs with increasing spin parameter a (0, 0.5, 0.9 and 0.9999). From left to right the columns correspond to different values of the magnetization parameter, namely non-magnetized ($\beta_{mc} = 10^{10}$), mildly magnetized ($\beta_{mc} = 1$) and strongly magnetized ($\beta_{mc} = 10^{-10}$)

Using this, we can write equation (A1) as

$$d\sigma^2 = e^{2F_1} d\theta^2 \left(\frac{r'^2}{N} + r^2 \right) + e^{2F_2} r^2 \sin^2 \theta d\phi^2, \quad (\text{A2})$$

with the prime ' denoting partial differentiation with respect to θ . Then, we try the embedding in \mathbb{E}^3 with the Cartesian metric $d\sigma^2 = dX^2 + dY^2 + dZ^2$ and the embedding functions:

$$X + iY = f(\theta) e^{i\phi}, \quad Z = g(\theta), \quad (\text{A3})$$

TABLE III. Disk parameters and values of their relevant physical magnitudes. For all the cases, we have $R_{\text{in}} = R_{\text{mb}}$ and $l = l_{\text{mb}}$

Model	l	W_c	R_{in}	R_c	β_{m_c}	h_{max}	ρ_{max}	p_{max}	$p_{m,\text{max}}$	R_{max}	$R_{m,\text{max}}$
I	0.934	-0.188	0.81	1.14	10^{10}	1.21	1.0	5.16×10^{-2}	5.50×10^{-12}	1.14	1.26
					1	1.10	1.17	3.11×10^{-2}	2.68×10^{-2}	1.01	1.06
					10^{-10}	1.0	1.90	1.10×10^{-11}	7.80×10^{-2}	0.93	0.96
II	0.933	-0.205	0.75	1.18	10^{10}	1.23	1.0	5.69×10^{-2}	6.14×10^{-12}	1.18	1.36
					1	1.12	1.19	3.50×10^{-2}	2.97×10^{-2}	1.00	1.07
					10^{-10}	1.0	2.01	1.30×10^{-11}	8.99×10^{-2}	0.91	0.94
III	1.06	-0.362	0.84	1.07	10^{10}	1.44	1.0	0.109	1.21×10^{-11}	1.07	1.22
					1	1.23	1.28	7.22×10^{-2}	5.76×10^{-2}	0.95	0.99
					10^{-10}	1.0	2.74	3.48×10^{-11}	0.206	0.89	0.91
IV	1.16	-0.547	0.67	1.06	10^{10}	1.723	1.0	0.182	2.09×10^{-11}	1.06	1.34
					1	1.38	1.37	0.129	9.76×10^{-2}	0.85	0.91
					10^{-10}	1.0	3.70	7.83×10^{-11}	0.408	0.76	0.78
V	1.20	-0.685	0.58	1.07	10^{10}	1.98	1.0	0.246	2.76×10^{-11}	1.07	1.31
					1	1.51	1.40	0.178	0.132	0.78	0.87
					10^{-10}	1.0	4.26	1.18×10^{-10}	0.579	0.67	0.69
VI	1.20	-0.832	0.43	1.12	10^{10}	2.30	1.0	0.324	3.52×10^{-11}	1.12	1.32
					1	1.66	1.39	0.228	0.169	0.72	0.86
					10^{-10}	1.0	4.54	1.57×10^{-10}	0.740	0.55	0.59
VII	0.920	-1.236	0.18	1.10	10^{-10}	3.44	1.0	0.610	6.459×10^{-11}	1.10	1.25
					1	2.25	1.64	0.510	0.322	0.43	0.62
					10^{-10}	1.0	10.42	7.03×10^{-10}	2.44	0.28	0.30

TABLE IV. Disc parameters and values of their relevant physical magnitudes for the KBH case. For all the cases, we have $R_{\text{in}} = R_{\text{mb}}$, $l = l_{\text{mb}}$ and $M_{\text{BH}} = 1$.

a	l	W_c	R_{in}	R_c	β_{m_c}	h_{max}	ρ_{max}	p_{max}	$p_{m,\text{max}}$	R_{max}	$R_{m,\text{max}}$
0	4.00	-4.32×10^{-2}	4.00	10.47	10^{10}	1.04	1.0	1.10×10^{-2}	1.15×10^{-12}	10.47	11.86
					1	1.02	1.11	6.29×10^{-3}	5.69×10^{-3}	8.81	9.52
					10^{-10}	1.0	1.48	1.83×10^{-12}	1.48×10^{-2}	7.70	8.14
0.5	3.41	-6.35×10^{-2}	2.99	7.12	10^{10}	1.07	1.0	1.64×10^{-2}	1.72×10^{-12}	7.19	8.14
					1	1.03	1.12	9.43×10^{-3}	8.47×10^{-3}	6.05	6.53
					10^{-10}	1.0	1.53	2.81×10^{-12}	2.23×10^{-2}	5.29	5.59
0.9	2.63	-0.129	2.18	3.78	10^{10}	1.14	1.0	1.64×10^{-2}	3.65×10^{-12}	3.78	4.23
					1	1.07	1.14	2.03×10^{-2}	1.78×10^{-2}	3.25	3.47
					10^{-10}	1.0	1.70	6.54×10^{-12}	4.92×10^{-2}	2.92	3.04
0.9999	2.02	-0.429	2.00015	2.034	10^{10}	1.54	1.0	0.134	1.61×10^{-11}	2.034	2.094
					1	1.29	1.51	0.110	7.52×10^{-2}	2.0075	2.014
					10^{-10}	1.0	6.17	1.22×10^{-10}	0.491	2.0021	2.0030

then

so we can write g'^2 as

$$g'^2 = e^{2F_1} \left(\frac{r'^2}{N} + r^2 \right) - e^{2F_2} (F'_2 r \sin \theta + r' \sin \theta + r \cos \theta)^2. \quad (\text{A5})$$

This result tells us that the r.h.s. of (A5) must be ≥ 0 in order to the embedding function to exist.

$$f = e^{2F_2} r^2 \sin^2 \theta, \quad f'^2 + g'^2 = e^{2F_1} \left(\frac{r'^2}{N} + r^2 \right), \quad (\text{A4})$$

Appendix B: Finding l_{mb} and r_{mb}

SG: To do.

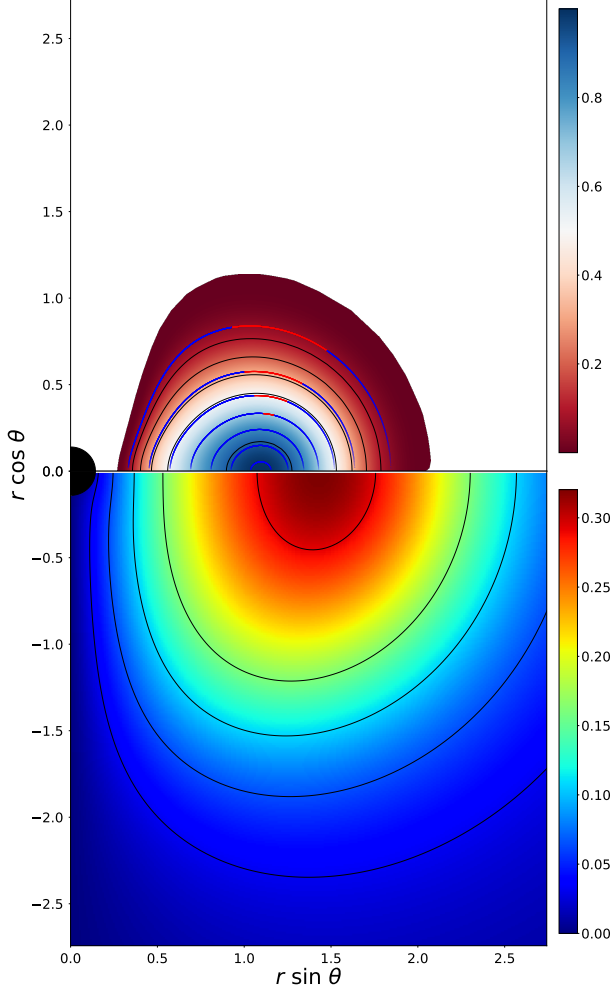


FIG. 11. Rest-mass density distribution for model VII with $r_{\text{in}} = 0.08$ and $\beta_{\text{mc}} = 10^{10}$ (up) and the scalar field amplitude distribution ϕ (down). The isocontours are blue when the r.h.s. of equation (A5) is > 0 and red when is ≤ 0 .